Nitroxide-Substituted Phenylphosphonic Acid: A New Building Block for the Design and Study of Magnetic Layered Materials

Philippe Gerbier, Christian Guérin,* Jean Le Bideau, and Karine Vallé

U.M.R. 5637 Chimie Moléculaire et Organisation du Solide, Université Montpellier II, Sciences et Techniques du Languedoc, Case 007, Place Eugène Bataillon, 34095 Monpellier Cedex 5, France

Received September 6, 1999
Revised Manuscript Received November 19, 1999

A growing interest in molecular magnetism[1−7] shed a peculiar light on magnetic studies carried out on metal phosphonates. These compounds are hybrid organic−inorganic solids that mostly possess layered structures.[8,9] The structural orthogonalization of the organic moieties with regard to the inorganic network provides a class of layered magnetic materials in which magnetic interactions within and between the inorganic layers can be varied through changes in the nature of either the metal cation or the organic component.[10−12] Despite their 2D dimensionality, antiferromagnetic interactions with long-range ordering have been reported in several cases.[11−18] To improve interlayer magnetic coupling, organic paramagnetic carriers[19,20] covalently bonded to the inorganic layers could be attractive candidates. Persistent aminoxyl radicals that are known to display interesting magnetic properties in the solid state can be used. For this purpose, our own approach was to develop phosphonic-based molecules bearing one *tert*-butyl nitroxide radical as building blocks to layered metal phosphonates. We report therein the synthesis and the magnetic properties of this new class of materials.

Scheme 1[a]

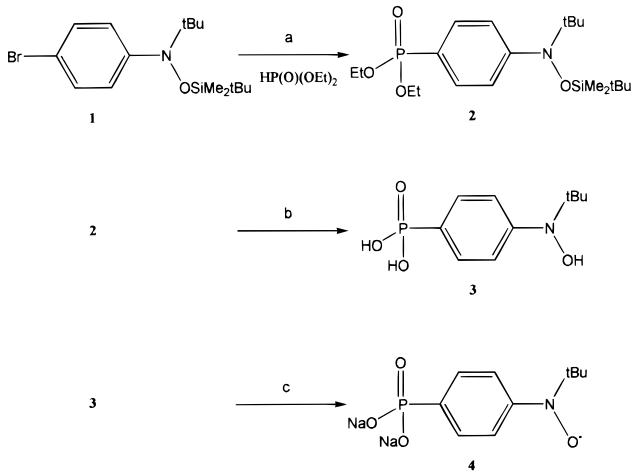

[a] Reaction conditions: (a) $C_6H_5CH_3$, $Pd(PPh_3)_4/Et_3N$, reflux for 4 h; (b) Me_3SiBr, CH_2Cl_2, 20 h, then H_2O; and (c) aqueous NaOH, PbO_2, 24 h.

The first step of the strategy we present here consists of the synthesis of the organic building block **4** as described in Scheme 1.[21] The bromo-4-[-*N*-*tert*-butyl-*N*-*tert*-butyldimethylsilyloxy]aniline **1** was condensed with diethyl phosphite using the Hirao procedure[22] to afford the TBDMS-protected diethylphosphonate **2**. The subsequent cleavage of ethyl ester with 3 equiv of trimethylsilyl bromide followed by hydrolysis gave the monohydrated acid **3** as a white powder. Its oxidation was performed as its sodium salt in aqueous solution with PbO_2, and the achievement of the reaction was checked by ^{1}H NMR spectroscopy. Removal of the solids by filtration led to a deep red solution from which **4** was

(1) Fegy, K.; Luneau, D.; Ohm, T.; Paulsen, C.; Rey, P. *Angew. Chem., Int. Ed. Engl.* **1998**, *37*, 1270.
(2) Nakatsuji, S.; Anzai H. *J. Mater. Chem.* **1997**, *7*, 2161.
(3) Ouahab, L. *Chem. Mater.* **1997**, *9*, 1909.
(4) Kahn, O.; Pei, Y.; Journaux, Y. In *Inorganic Materials*, 2nd ed.; Bruce, D. W.; O'Hare, D., Eds.; J. Wiley & Sons: New York, 1997, p 65.
(5) Miller, J. S.; Epstein, A. J. *Angew. Chem., Int. Ed. Engl.* **1994**, *33*, 385.
(6) Kahn O., Ed. *Molecular Magnetism*; VCH: New York, 1993.
(7) Benelli, C.; Gatteschi, D. *Coord. Chem. Rev.* **1992**, *120*, 137.
(8) Alberti, G.; Casciola, M.; Costantino, U.; Vivani, R. *Adv. Mater.* **1996**, *8*, 291.
(9) Clearfield, A. In *Progress in Inorganic Chemistry*; Karlin, K. D., Ed.; J. Wiley & Sons: New York, 1998; Vol. 47, p 371.
(10) Le Bideau, J.; Papoutsakis, D.; Jackson, J. E.; Nocera, D. G. *J. Am. Chem. Soc.* **1997**, *119*, 1313.
(11) Carling, S. G.; Day, P.; Visser, D. *J. Phys.: Condens. Matter* **1995**, *7*, L109.
(12) Le Bideau, J.; Payen, C.; Bujoli, B.; Palvadeau, P.; Rouxel, J. *J. Magn. Magn. Mater.* **1995**, *140−144*, 1719.
(13) Huan, G.; Johnson, J. W.; Brody, J. F.; Goshorn, D. P. *Mater. Chem. Phys.* **1993**, *35*, 199.
(14) Seip, C. T.; Byrd, H.; Talham, D. R. *Inorg. Chem.* **1996**, *35*, 3479.
(15) Seip, C. T.; Granroth, G. E.; Meisel, M. W.; Talham, D. R. *J. Am. Chem. Soc.* **1997**, *119*, 7084.
(16) Fanucci, G. E.; Krzystek, J.; Meisel, M. W.; Brunel, L. C.; Talham, D. R. *J. Am. Chem. Soc.* **1998**, *120*, 5469.
(17) Bellito, C.; Federici, F.; Ibrahim, S. A. *Chem. Mater.* **1998**, *10*, 1076.
(18) Rabu, P.; Janvier, P.; Bujoli, B. *J. Mater. Chem.* **1999**, *9*, 1323.
(19) Stumpf, H. O.; Ouahab, L.; Pei, Y.; Bergerat, P.; Kahn, O. *J. Am. Chem. Soc.* **1994**, *116*, 3866.
(20) Laget, V.; Hornick, C.; Rabu, P.; Drillon, M.; Turek, P.; Ziessel, R. *Adv. Mater.* **1998**, *10*, 1024.

(21) The bromo-4-[-*N*-*tert*-butyl-*N*-*tert*-butyldimethylsilyloxy]aniline **1** was prepared according to the procedure described by: Inoue, K.; Iwamura, H. *Angew. Chem., Int. Ed. Engl.* **1995**, *34*, 927. **2**: A solution of **1** (13.9 mmol, 5 g), diethyl phosphite (15.3 mmol, 2.1 mL), triethylamine (15.9 mmol, 2.04 mL), and $Pd(PPh_3)_4$ (0.7 mmol, 0.81 g) in toluene (20 mL) was heated at 90 °C for 4 h under N_2. After the mixture was cooled, filtered, and evaporated in vacuo, the crude oily product was chromatographed (silica gel, ether) and gave compound **2** (4.9 g, 85%) as a colorless oil. **3**: A mixture of **2** (4.9 g, 11.8 mmol) and trimethylsilyl bromide (5 mL, 37.8 mmol) was stirred overnight in CH_2Cl_2 (50 mL) under N_2. The removal of the solvents in vacuo followed by the addition of a mixture of EtOH/H_2O (1/1) resulted in the formation of a white precipitate. The recrystallization from EtOH gave a white solid **3** (2.6 g, 90%). ^{1}H NMR (200 MHz, DMSO-d^6): δ 1.10 (s, 9H, Bu^t); 7.27 (dd, 2H, Ph, $^3J_{HH} = 8.5$ and $^4J_{HP} = 3.2$); 7.56 (dd, 2H, Ph, $^3J_{HH} = 8.5$ and $^3J_{HP} = 12$, 3); 8.45 (s, 1H, N(O*H*)). ^{31}P NMR (81 MHz, DMSO-d^6): δ 14.5. ^{13}C NMR (50 MHz, DMSO-d^6): δ 26.8 (s, $(CH_3)_3$CN); 60.9 (s, $(CH_3)_3C$N); 124.1 (d, Ph, $^2J_{CP} = 14.7$); 129.6 (d, Ph, $^1J_{CP} = 190.5$); 130.7 (d, Ph, $^3J_{CP} = 15.3$); 153.8 (s, Ph). Anal. Calcd for $C_{10}H_{16}NO_4P\cdot H_2O$ (found): C, 45.8 (45.22); H, 6.87 (6.87); N, 5.34 (5.24); O, 30.5 (29.61); P, 11.83 (11.83). **4**: **3** (1 g, 3.8 mmol) was neutralized with a NaOH solution (7.6 mL, 1 M) and subsequently oxidized with PbO_2 (1.5 g, 6.3 mmol) overnight. The resulting mixture was filtered through Celite and evaporated in vacuo to yield an orange hygroscopic solid **4** (1.27 g, 98%). Anal. Calcd for $C_{10}H_{13}NNa_2O_4P\cdot 3\ H_2O$ (found): C, 35.09 (35.63); H, 5.55 (5.11); N, 4.09 (4.19); Na, 13.45 (13.24); P, 9.06 (9.37).

(22) Hirao, T.; Masunaga, T.; Ohshiro, Y.; Agawa, T. *Synthesis* **1981,** *1*, 56.

10.1021/cm991139f CCC: $19.00
Published on Web 01/25/2000

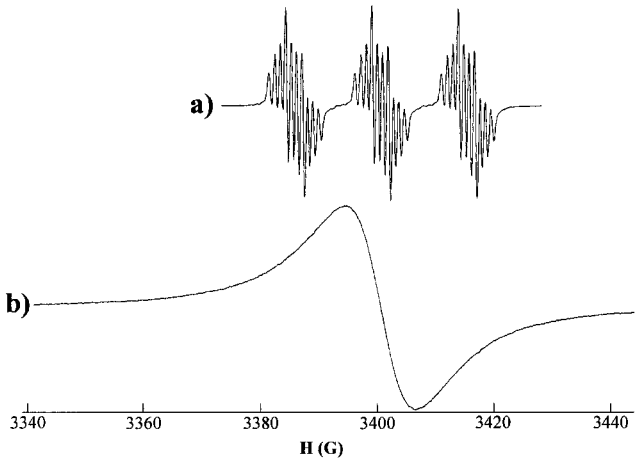

Figure 1. EPR spectra of the phosphonate radical **4** (a) in a 10^{-4} M aqueous solution and (b) in the solid-state at 298 K.

Scheme 2[a]

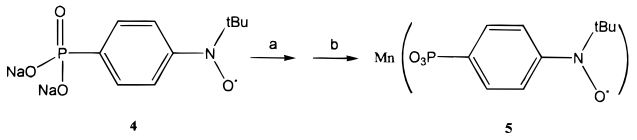

[a] Reaction conditions: (a) HCl/H_2O; (b) $MnSO_4/H_2O$, then pH = 6, reflux for 24 h.

recovered as an orange hygroscopic powder after evaporation of the solvent under reduced pressure.

The powder X-ray diffraction pattern is characteristic of a layerlike structure; the strong intensity of the first line could thus be attributed to an interlayer distance of 22.7 Å. The structure collapses as the phosphonate absorbs the ambient atmospheric humidity. The ESR spectrum (Figure 1a) of a 10^{-4} M aqueous solution of **4** shows the characteristic triplet due to the nitrogen splitting in the *tert*-butyl nitroxide radicals ($g = 2.008$ and $|a_N| = 14.7$ G). The hyperfine coupling in the triplet displays a 10-line pattern originating from the interactions of the nitroxide radical with the ortho ($|a_H| = 14.7$ G) and meta ($|a_H| = 0.9$ G) hydrogen nuclei as well as the para phosphorus atom ($|a_P| = 3.2$ G). In the solid state (Figure 1b), a narrow single signal ($\Delta H_{pp} = 12$ G) is observed at $g = 2.008$ at room temperature. No half-field transitions are observed in the spectrum down to 4 K.

The synthesis of the organic−inorganic hybrid material $Mn[O_3PC_6H_4N(O^{\bullet})tBu]\cdot H_2O$ **5** was outlined in Scheme 2.[23] An aqueous solution of **4** was added to an equimolar solution of $MnSO_4$; the pH was further increased to 6 in order to ensure complete precipitation of the solid. Besides the elemental analysis data (see Experimental Section), the $Mn^{2+}/NO^{\bullet}$ ratio was confirmed as follows. The ESR spectrum of a freshly prepared solution of **5** in 2 M aqueous HCl displays the superimposition of a broad sextet characteristic of the Mn(II) solvated ions and of a sharp triplet attributed to the aminoxyl radical moieties. A simulation of the above spectrum has yielded a $Mn^{2+}/NO^{\bullet}$ ratio of ca. 0.94.

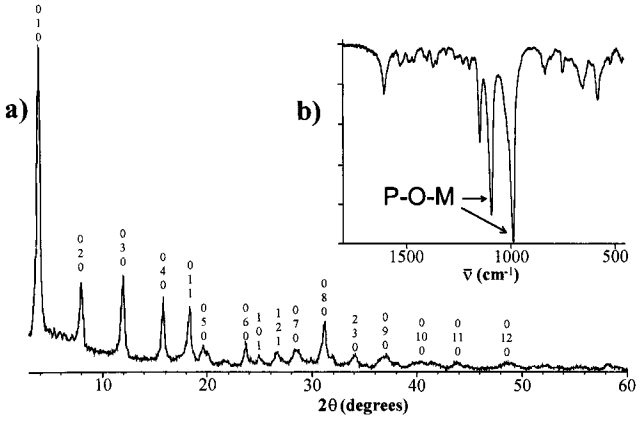

Figure 2. (a) Powder XRD pattern and (b) IR spectrum (KBr pellets) of $Mn[O_3PC_6H_4N(O^{\bullet})tBu]\cdot H_2O$ **5**.

The X-ray powder diffraction profile for **5** (Figure 2a) is characteristic of a preferred orientation induced by a layered structure. The indexation was carried out by using the Ito methods,[24] starting from the 29 observed lines of the XRD pattern, and gave an orthorhombic system with the following cell parameters: $a = 5.78(1)$ Å, $b = 22.32(6)$ Å, and $c = 4.99(1)$ Å. The a and c parameters that feature the inorganic layer are in agreement with those found for the known $Mn(O_3PC_6H_5)\cdot H_2O$.[25] Additionally, the infrared spectra of these two compounds are quite similar in the PO_3M region[15] (Figure 2b). The similarities of the XRD patterns and IR results for this phase and $Mn(O_3PC_6H_5)\cdot H_2O$ permit us to propose a similar crystal structure without a significant variation of the manganese phosphonate sheets. The observed increase of the interlayer distance for **5** (22.32 vs 14.33 Å for $Mn(O_3PC_6H_5)\cdot H_2O$) is consistent with the replacement of the para hydrogen atom by the sterically demanding *t*Bu-$NO^{\bullet}$ group on the phenyl ring (Figure 3).[26]

Variable-temperature magnetic susceptibility measurements have been carried on a VSM susceptometer in the temperature range of 2−300 K with an applied field of 0.5 T. The $\chi_m T$ versus T plot for compound **4** (Figure 4) indicated predominant antiferromagnetic interactions, with a Weiss constant $\theta_P = -4.4$ K. From the high-temperature region (150−300 K), the spin concentration was estimated to be 0.86 radical spin per mole of **4.** This value, which is lower than the expected one, may be explained by a slight hydration during the sampling (vide supra). For the compound **5** (Figure 5), a quite different magnetic behavior is noticed. As observed for the sodium salt **4**, predominant antiferromagnetic interactions exist in **5**, and the Weiss constant θ_P obtained from the Curie−Weiss region (150−300 K) is −43 K. On the other hand, in contrast to **4**, the disruption in the χ_m versus T curve (Figure 5a) at lower

(23) **5**: 40 mL of an aqueous solution of **4** (1.1 g, 3.8 mmol) was acidified with HCl (3.8 mL, 1 M) and $MnSO_4\cdot H_2O$ (0.64 g, 3.8 mmol) was added. The precipitation of the expected material **5** was obtained by making the pH = 6 with a NaOH solution. After filtration and washing, **5** is refluxed in H_2O for 24 h to yield a brown powder (1.10 g, 92%). Anal. Calcd for $C_{10}H_{13}MnNO_4P\cdot H_2O$ (found): C, 38.10 (36.33); H, 4.13 (4.72); Mn, 17.44 (17.60); N, 4.44 (4.13); P, 9.84 (10.19); IR (KBr): ν [cm^{-1}] = 3507, 3433 ($\nu(H_2O)$), 1602 ($\delta(H_2O)$), 1089($\nu_a(PO_3)$), 987($\nu_s(PO_3)$), 574 ($\delta(PO_3)$).

(24) Visser, J. W. *J. Appl. Crystallogr.* **1969**, *2*, 89.

(25) Cao, G.; Lee, H.; Lynch, V. M.; Mallouk, T. E.; *Inorg. Chem.* **1988**, *27*, 2781.

(26) The idealized structure has been built up by combining crystallographic data of $Mn(O_3PC_6H_5)\cdot H_2O$ and some 4-[$C_6H_4N(O^{\bullet})$-*t*Bu] groups obtained from the Cambridge Crystallographic Database and optimized in order to agree with the experimental powder XRD data.

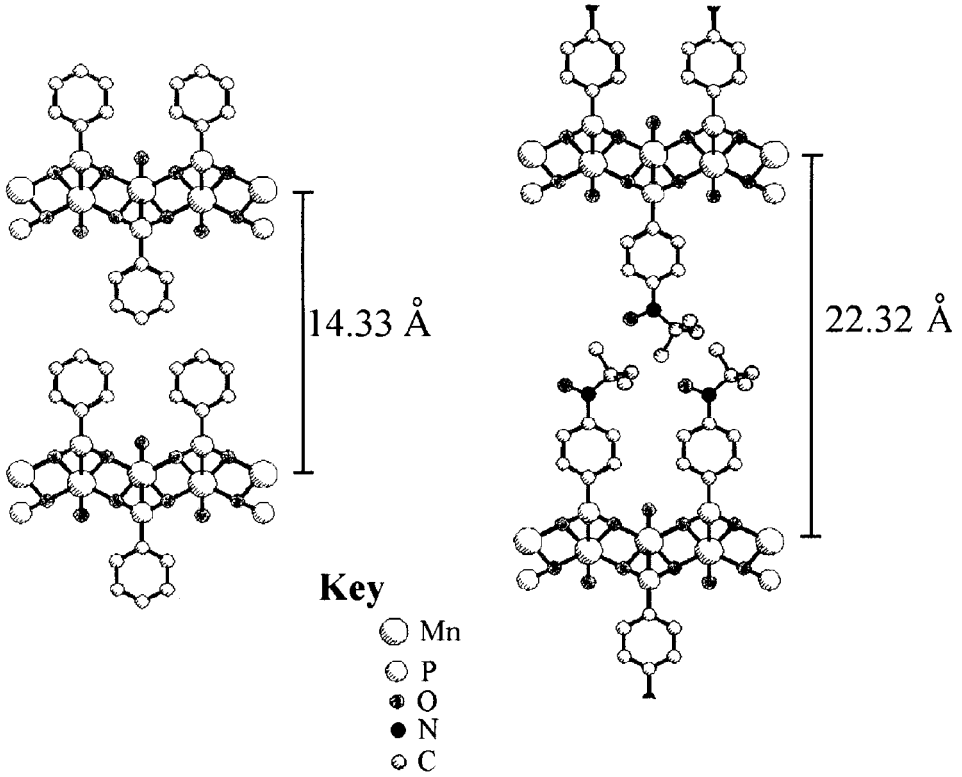

Figure 3. (a) Crystal structure of $Mn(O_3PC_6H_5)\cdot H_2O$ and (b) idealized structure of $Mn[O_3PC_6H_4N(O^{\bullet})tBu]\cdot H_2O$ **5**.

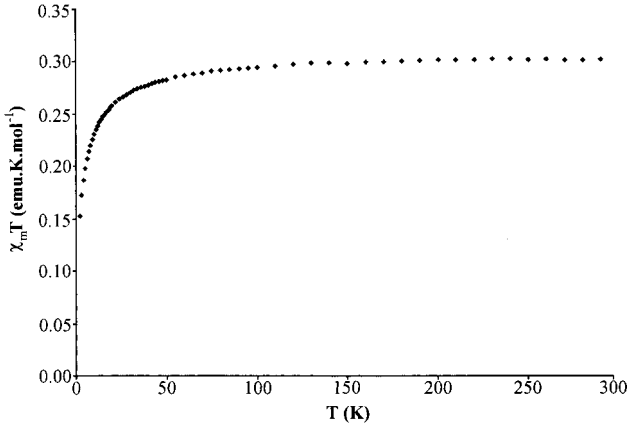

Figure 4. Thermal variation of $\chi_m T$ for **4**.

temperatures is indicative of a 3D antiferromagnetic ordering (T_N = 12 K). The broad paramagnetic maximum around 19 K is characteristic of a low-dimensional antiferromagnetism. Moreover, it is noteworthy that the $\chi_m T$ versus T curve (Figure 5b) shows a continuous fall from 300 to 2 K. Thus, the experimental effective moment should be lower than expected for noninteracting paramagnetic centers. The $\chi_m T$ value obtained at room temperature, 3.88 emu K mol^{-1} (μ_{eff} = 5.57 μ_B), is effectively lower than expected for one Mn(II) and one organic radical isolated spin carriers spins, ca. 4.74 emu K mol^{-1} (μ_{eff} = 6.15 μ_B).

ESR solid-state spectra of **5** at temperatures ranging from 300 to 4 K are given in Figure 6. At room temperature, the spectrum displays a single broad resonance at g = 2.0010, as it is generally reported in the literature for Mn^{II} phosphonates[14,27] or Mn^{II} nitrox-

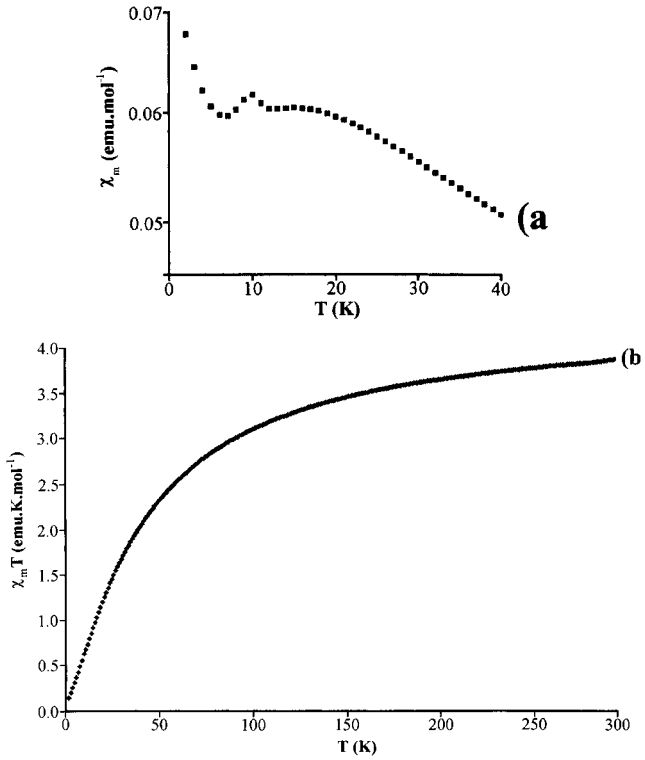

Figure 5. Thermal variation of (a) χ_m and (b) $\chi_m T$ for **5**.

ide complexes.[28,29] The line width (ΔH_{pp} = 186 G) is smaller than the observed value for the manganese phenylphosphonate (ΔH_{pp} = 215 G).[27] The area of the EPR signal gradually increases with decreasing tem-

(27) Byrd, H.; Pike, J. K.; Talham, D. R. *Synth. Met.* **1995**, *71*, 1977.

(28) Caneschi, A.; Gatteschi, D.; Laugier, J.; Rey, P.; Zanchini, C. *Inorg. Chem.* **1988**, *27*, 2027.

(29) Caneschi, A.; Gatteschi, D.; Renard, J. P.; Rey, P.; Sessoli, R. *Inorg. Chem.* **1990**, *28*, 1976.

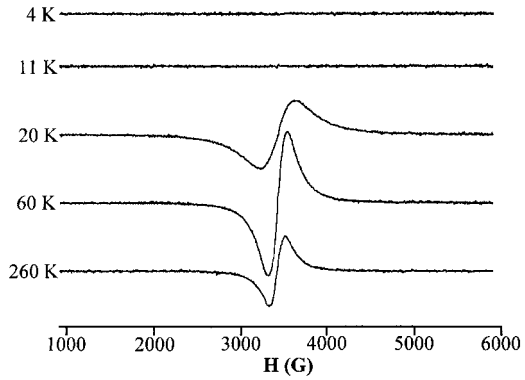

Figure 6. Solid-state EPR spectra of **5** at different temperatures.

perature and reaches a maximum near 20 K, which is accompanied by a significant line width broadening. Such a behavior is characteristic of short-range antiferromagnetic fluctuations in 2D networks.[14] The signal abruptly disappears around 12 K, which is in accordance with the observed magnetic transition in the magnetization curve (vide supra). Below this temperature, no appreciable signal can be noticed in the spectrum and no additional feature is observed at half-field. No signals corresponding to the nitroxide radicals are observed.

From the above data, one can conclude, first, that the magnetic behaviors of **4** and **5** differ significantly. As shown for the sodium salt **4**, a layered ionic structure only provides small antiferromagnetic interactions between the spin carriers. Changing the nature of the cation (Mn^{2+}, **5**), we have prepared a more covalent layered structure in which a 3D antiferromagnetic ordering occurs at low temperature. Second, it appears that the magnetic behavior of **5** and of the related manganese phenylphosphonates[12,16,30] are rather similar: as observed previously for isotype *n*-alkylphosphonates, drastic variations in the interlayer distance did not affect T_N.[14−16,31] Moreover, if we consider that the structures of both **5** and the manganese phenylphosphonate are similar, it appears that the *p*-[*tert*-butylnitroxide]-phenyl radicals did not cause substantial electron-donating changes in the inorganic layers.[10]

Finally, a long-range magnetic ordering in a structurally 2D compound raises the question of a truly 2D magnetic network with anisotropic exchanges, or of a magnetic system with interlayer interactions, thus allowing the hypothesis of isotropic exchanges. In the case of the phosphonates, the independence of the Néel temperature T_N on the interlayer distance is in favor of a real 2D magnetic network. On the other hand, although divalent manganese is known to undergo isotropic interactions, previous antiferromagnetic resonance (AFMR) studies carried out on manganese phosphonates have shown some magnetic anisotropy in the magnetically ordered state.[16] This result is in accordance with the T_N dependence upon diamagnetic dilution in the case of 2D antiferromagnetic networks as shown elsewhere.[15,32,33] We have shown here that the presence of a spin carrier between the metal-based sheets (6.6 Å apart from the closest layer, 7 Å from the closest Mn atom) did not modify the bulk magnetic behavior, which confirms the truly 2D character of the magnetic network. Thus, anisotropic exchanges within the layers appear to be essential for the setting up of the 3D magnetic ordering. Nevertheless, although the magnetic susceptibility data do not provide any information on the role of the organic nitroxide radicals, the ESR results suggest the possibility of a magnetic ordering of the latter induced by the inorganic layers. From this respect, efforts are currently being made in the synthesis and magnetic study of similar compounds with other transition-metal ions.

Acknowledgment. We gratefully acknowledge Dr. B. Deroide for his help in ESR spectra interpretation and simulation, as well as the S3M magnetometer facility of the Université Montpellier II.

CM991139F

(30) Cunningham, D.; Hennelly, P. J. D.; Deeney, T. *Inorg. Chim. Acta* **1979**, *37*, 95.
(31) Le Bideau, J.; Payen, C.; Bujoli, B.; *C. R. Acad. Sci. Paris* **1995**, *320*, 141.
(32) Endoh, Y.; Yamada, K.; Birgeneau, R. J.; Gabbe, D. R.; Jenssen, H. P.; Kastner, M. A.; Peters, C. J.; Picone, P. J.; Thurston, T. R.; Tranquada, J. M.; Shirane, G.; Hidaka, Y.; Oda, M.; Enomoto, Y.; Suzuki, M.; Murakami, T. *Phys. Rev. B* **1988**, *37*, 7443.
(33) Visser, D.; Clarke, S. J.; Harrison, A. *J. Appl. Phys.* **1993**, *73*, 5397.